Lecture 1 . Dynamics of Structure formation and Statistical measures

Diego Garcia Lambas, IATE -
Observatorio Astrónomico. Córdoba Argentina.

Pedra Azul, Espirito Santo, September 2022

Isotropy and homogeneity at large scales

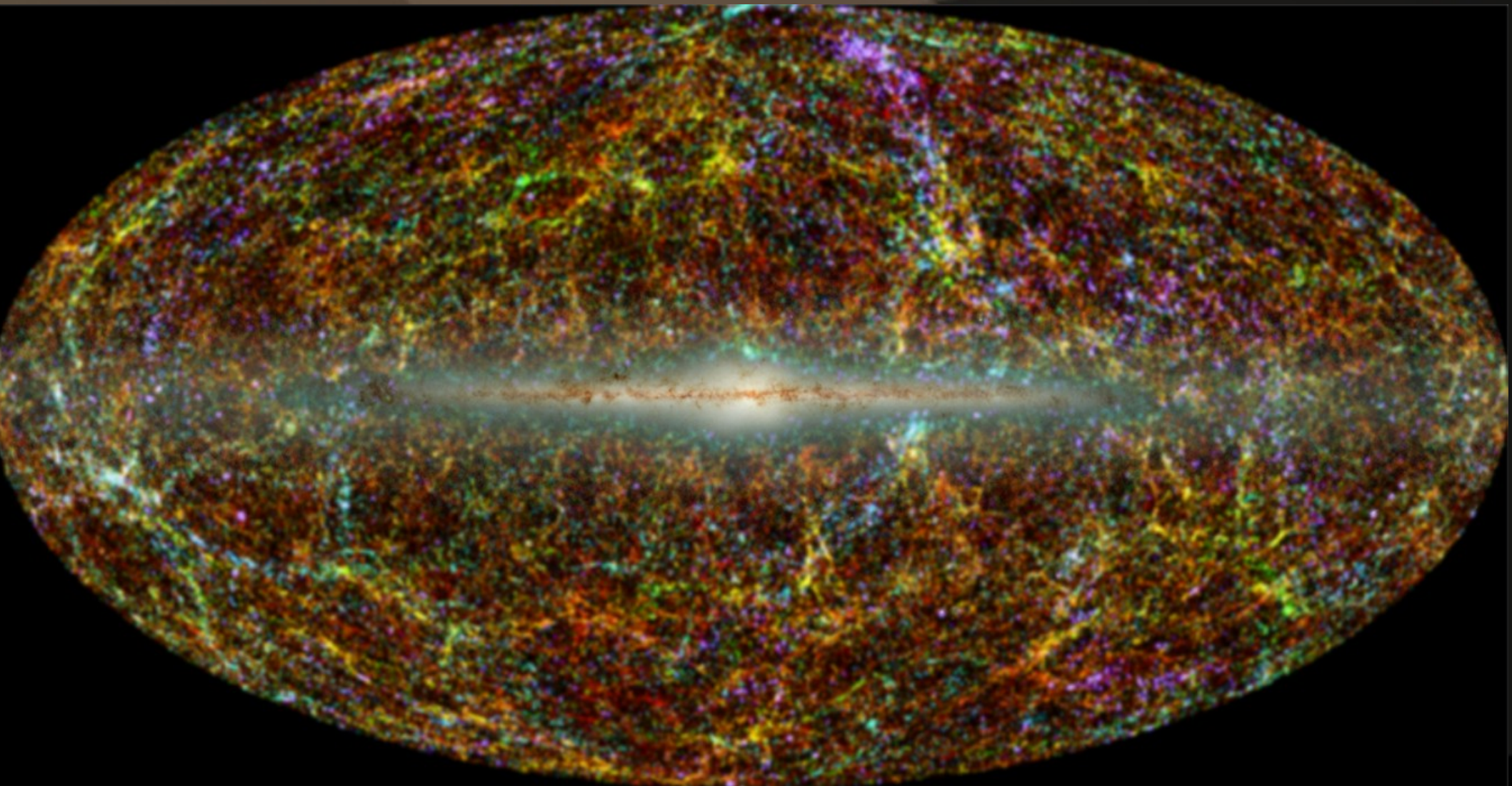

spatial homogenenity
a(t) coordinate strech
global dynamics

$$ds^2 = -(1+2\phi/c^2)c^2dt^2 + (1-2\phi/c^2)a^2(t)(dx_1^2 + dx_2^2 + dx_3^2$$

$$\left(\frac{\dot{a}}{a}\right)^2 = \frac{8\pi}{3}Ga^2\bar{\rho}(a) - K$$

$$\Omega(t) \equiv \frac{\bar{\rho}(t)}{\rho_c(t)} \equiv \frac{8\pi G\bar{\rho}(t)}{3H^2(t)}\,, \quad \rho_c(t_0) = 2\times 10^{-29}\,h^2\ \mathrm{g\ cm^{-3}}$$

- Global spatial isotropic (homogeneous at large scales).
    - Particle dynamics in expanding coordinates.
- Understanding structure using locally Newtonean dynamics.

Transformation to comoving coordinates

$$\mathbf{u} = a\dot{\mathbf{x}} + \mathbf{x}\dot{a},$$

Lagrangian in x-coordinates and transformation to remove cross term

$$\mathcal{L} = \tfrac{1}{2} m (a\dot{\mathbf{x}} + \dot{a}\mathbf{x})^2 - m\Phi(\mathbf{x}, t).$$

Peebles, 1980

$$\mathcal{L} \rightarrow \mathcal{L} - d\psi/dt, \qquad \psi = \tfrac{1}{2} m a \dot{a} x^2,$$

$$\phi = \Phi + \tfrac{1}{2} a\ddot{a}x^2$$

Equations for comoving potential

$$\nabla^2\phi = 4\pi G\rho a^2 + 3a\ddot{a}.$$

Perturbations are source of the new potential

$$\nabla^2\phi = 4\pi G a^2 [\rho(\mathbf{x}, t) - \rho_b(t)]$$

equation of motion in comoving cooordinates

$$\mathbf{p} = ma^2\dot{\mathbf{x}} \qquad \frac{d\mathbf{p}}{dt} = -m\nabla\phi$$

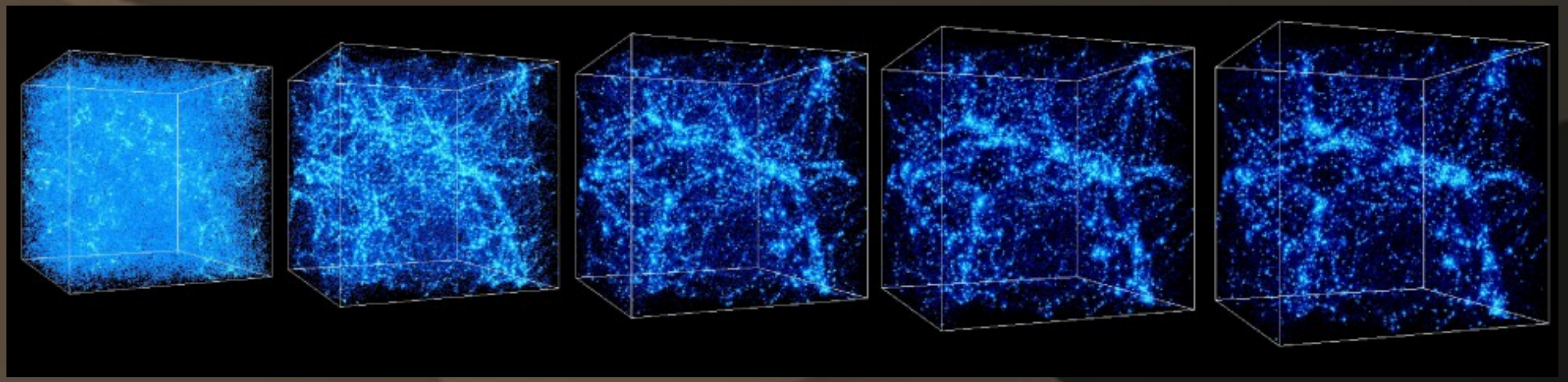

Evolution in a comoving box

$$\frac{d\vec{x}_i}{d\tau} = \vec{v}_i \ , \quad \frac{d\vec{v}_i}{d\tau} = -\frac{\dot{a}}{a}\vec{v}_i - \vec{\nabla}\phi \ , \quad \nabla^2\phi = 4\pi G a^2 \left[\sum_j m_j \delta_{\rm D}(\vec{x} - \vec{x}_i) - \bar{\rho}_m(\tau) \right]$$

Equations of Cosmological Hydrodynamics

Multispecies gas dynamics

Mass cons:
$$\frac{\partial \rho_b}{\partial t} + \vec{\nabla} \cdot (\rho_b \vec{v}_b) + 3\frac{\dot{a}}{a}\rho_b = 0,$$

Mom cons:
$$\frac{\partial (\rho_b v_{b,i})}{\partial t} + \vec{\nabla} \cdot [(\rho_b v_{b,i})\vec{v}_b] + 5\frac{\dot{a}}{a}\rho_b v_{b,i} = -\frac{1}{a^2}\frac{\partial p}{\partial x_i} - \frac{\rho_b}{a^2}\frac{\partial \phi}{\partial x_i},$$

Energy cons:
$$\frac{\partial e}{\partial t} + \vec{\nabla} \cdot (e\vec{v}_b) + p\vec{\nabla} \cdot \vec{v}_b + 3\frac{\dot{a}}{a}(e+p) = \Gamma - \dot{E},$$

Species cons:
$$\frac{\partial \rho_i}{\partial t} + \vec{\nabla} \cdot (\rho_i \vec{v}_b) + 3\frac{\dot{a}}{a}\rho_i = \pm \sum_j \sum_l k_{jl}(T)\rho_j \rho_l \pm \sum_j I_j \rho_j,$$

2-body reactions; photo-dissoc./ionization

Dark matter dynamics

Newton's law:
$$\frac{d\vec{x}_d}{dt} = \vec{v}_d,$$
$$\frac{d\vec{v}_d}{dt} = -2\frac{\dot{a}}{a}\vec{v}_d - \frac{1}{a^2}\vec{\nabla}\phi.$$

Poisson eq.
$$\nabla^2 \phi = 4\pi G a^2 (\rho - \bar{\rho}),$$

Metric

$$\frac{da}{dt} = H_0 \left[\Omega_M (\frac{1}{a} - 1) + \Omega_\Lambda (a^2 - 1) + 1\right]^{1/2}$$

Friedmann eq. for scale factor a(t)

D. Norman, AAS 2020

- The formation of galaxies in a cosmological context could in principle be simulated with reliability:

  Collisionless and gas dynamics can be accurately followed, difficulties arise when gas cooling is allowed → compacting gas clouds triggering star formation.

- Stellar astrophysics start playing a significant role :

  Phenomenological recipies for star formation. Resolution limitation of simulations .

  Complexity of the astrophysical processes (magenetic fields, microscopic physics, molecular gas, metal enrichment, etc.)

Astrophysical feedback physics:

Stellar winds, SN explosions, chemical enrichment effects on cooling.

+ BH feedback

DM only simulations + semianalytic models

RECIPY

- Galaxies are originated in dark matter halos
- Semianalytic model include different processes such as gas cooling, star formation, feedback, ram pressure stripping, stellar quenching, etc.

  - Constrained to reproduced main properties of galaxies

Semianalytic models

GIF simulations Colberg & Diaferio

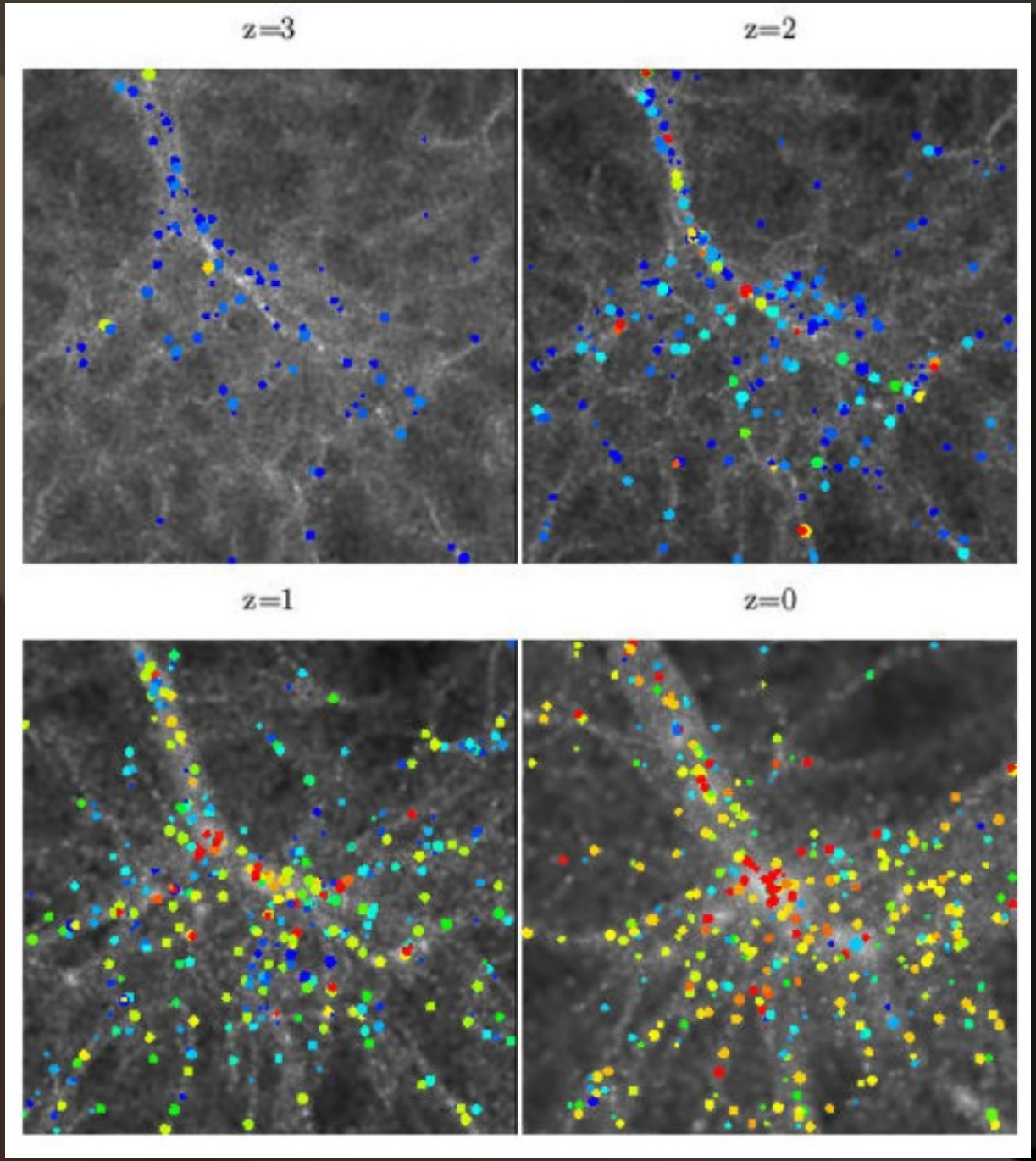

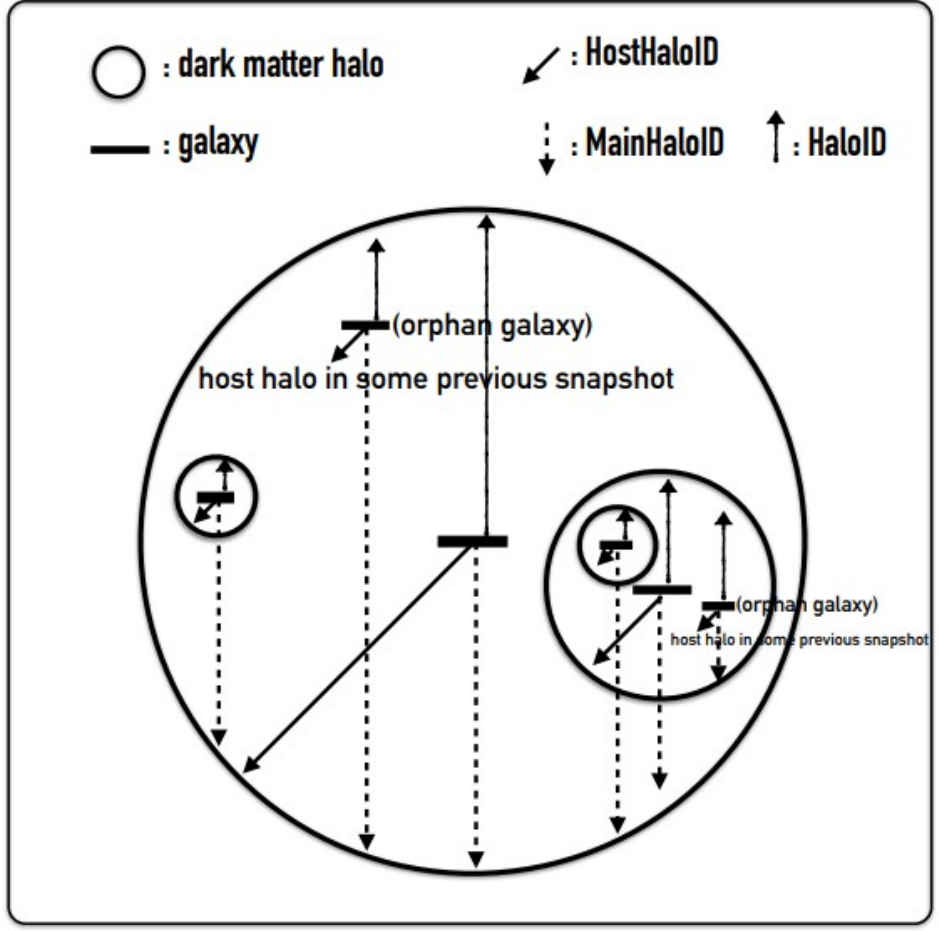

Figure A1. Illustrating the various pointers to haloes in which galaxies are residing.

Scheme of galaxy semi-analytic modelling

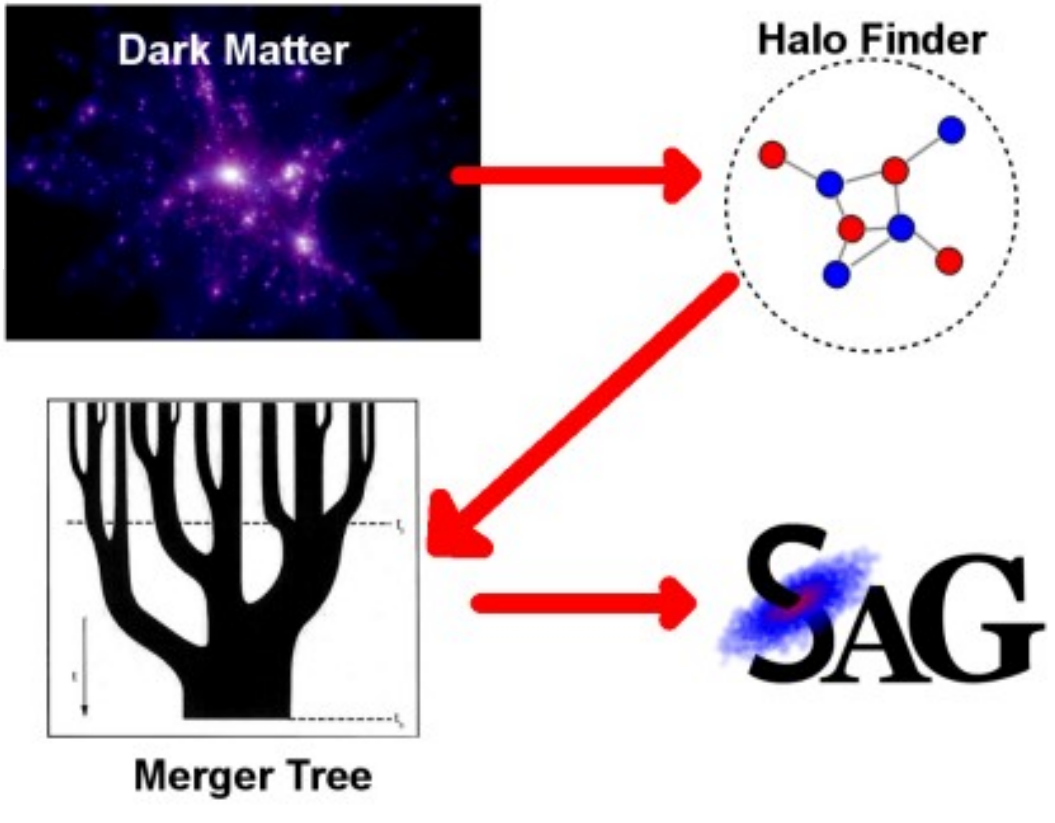

Analyzing structure with statistical methods

Galaxy groups and clusters, filaments, cosmic voids etc. require particular definitions

The nature of the galaxy distribution, can be adequately characterized through correlation functions/power spectrum.

$$\delta(\mathbf{x}) \equiv \frac{\rho(\mathbf{x}) - \langle\rho\rangle}{\langle\rho\rangle}$$

$$\xi(\mathbf{r}) \equiv \langle\delta(\mathbf{x})\delta(\mathbf{x}+\mathbf{r})\rangle$$

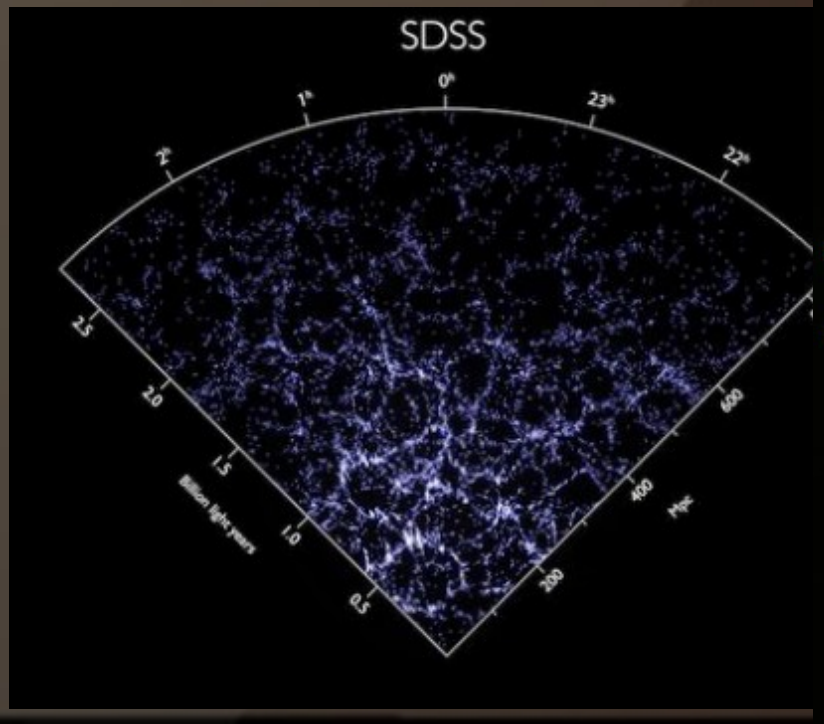

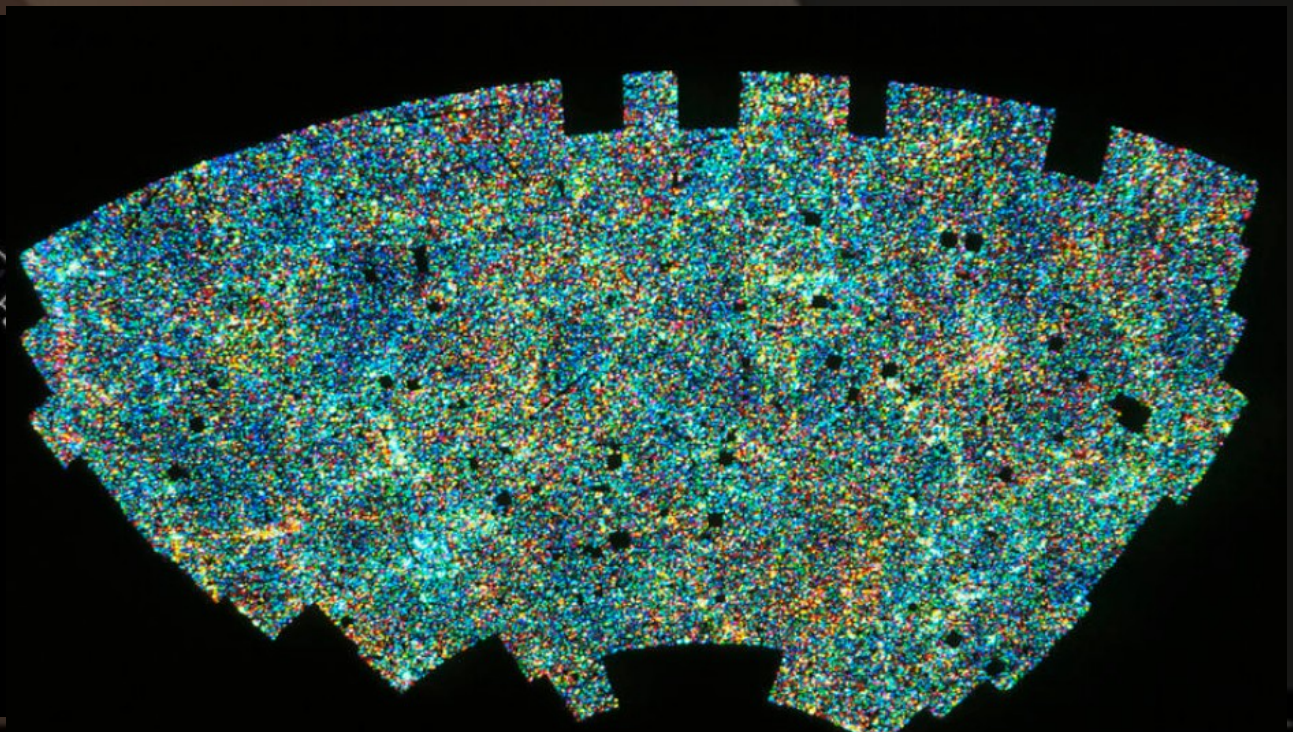

For a distribution of points:

D is the number of pairs in the data
R is the number of pairs in a random distribution

$$\xi \approx \frac{DD - 2DR + RR}{RR}$$

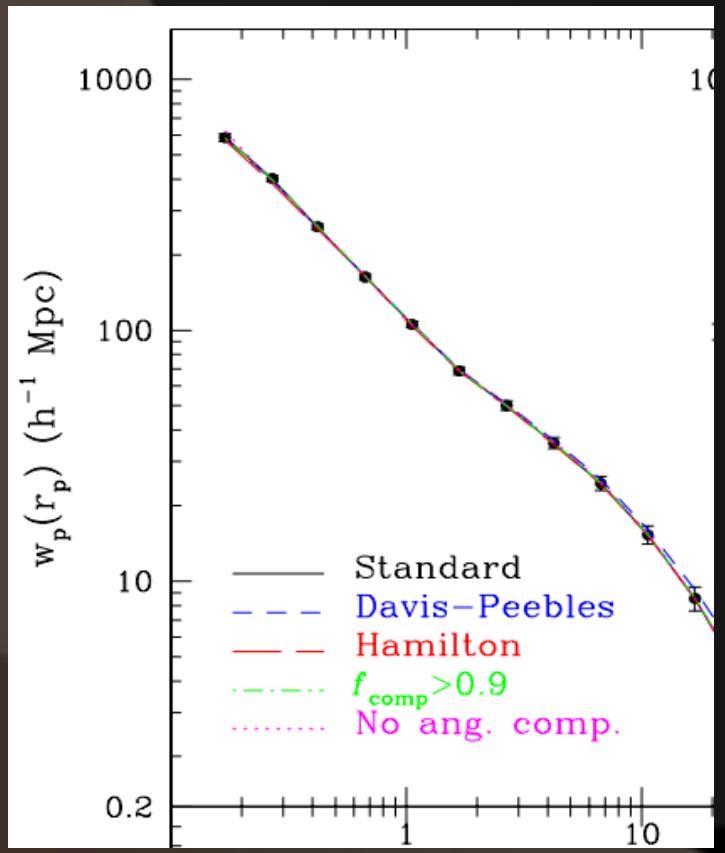

If the distribution of points is gaussian,
the whole characterization of the distribution
can be achieved with the two point function or PS.

The higher order correlations can be
expressed in terms of the TPCF : Hierarchical structure

The two halo term of the TPCF can be clearly seen in the simulations. (and in the Data)

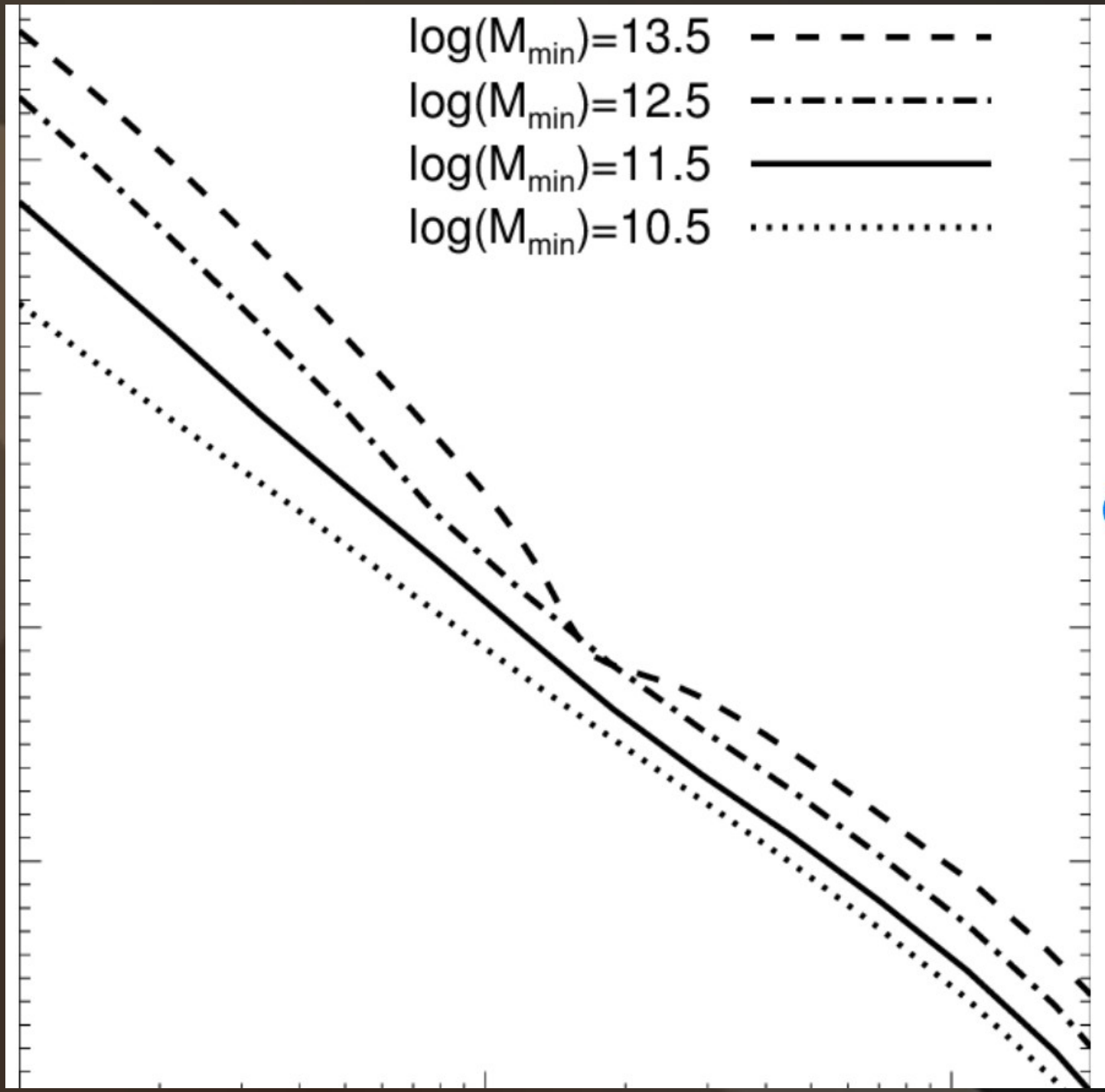

SDSS data

Zehavi et al. 2013

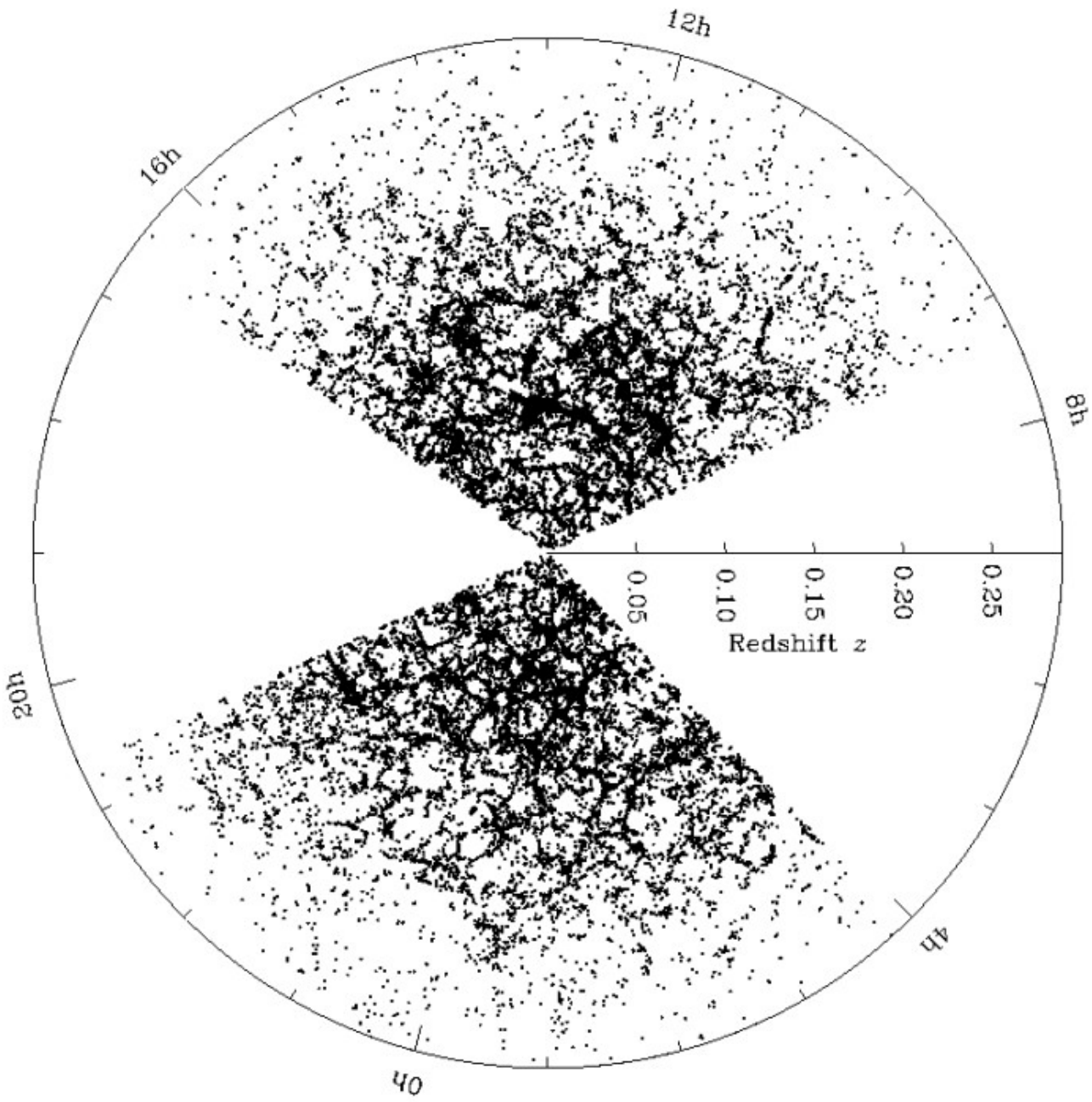

FIG. 1.— The distribution of galaxies in the SDSS main galaxy sample. Only galaxies within ±1.25 degrees of the Celestial Equator are shown.

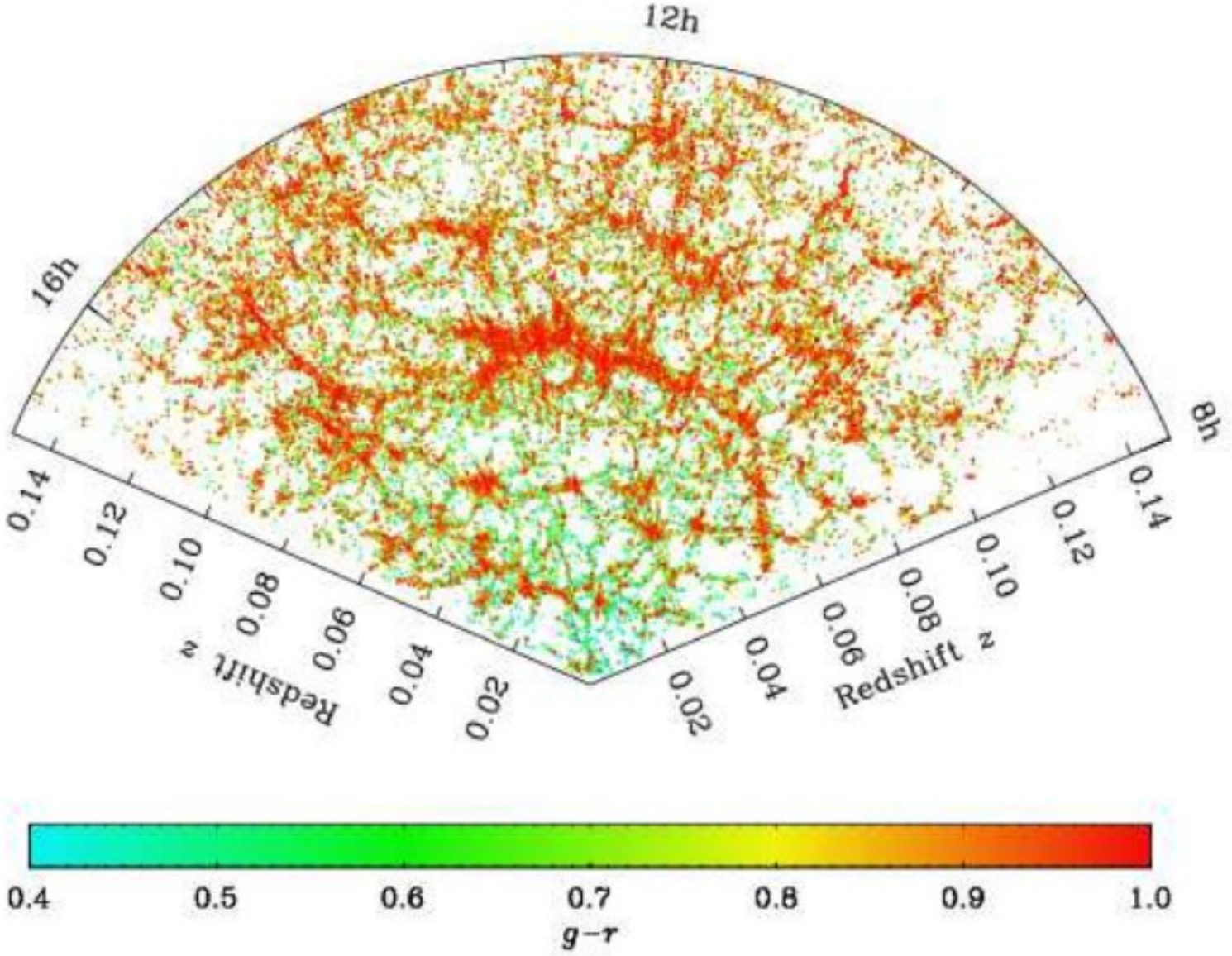

FIG. 2.— A slice through the SDSS main galaxy sample, with galaxies color-coded based on rest-frame $g - r$ color. The slice shows galaxies within ±4 degrees of the Celestial Equator, in the north Galactic cap. The redshift limit is smaller than in Figure 1 to better reveal details of structure. The large structure cutting across the center of the map is the "Sloan Great Wall" (Gott et al. 2005) discussed in §3.2.

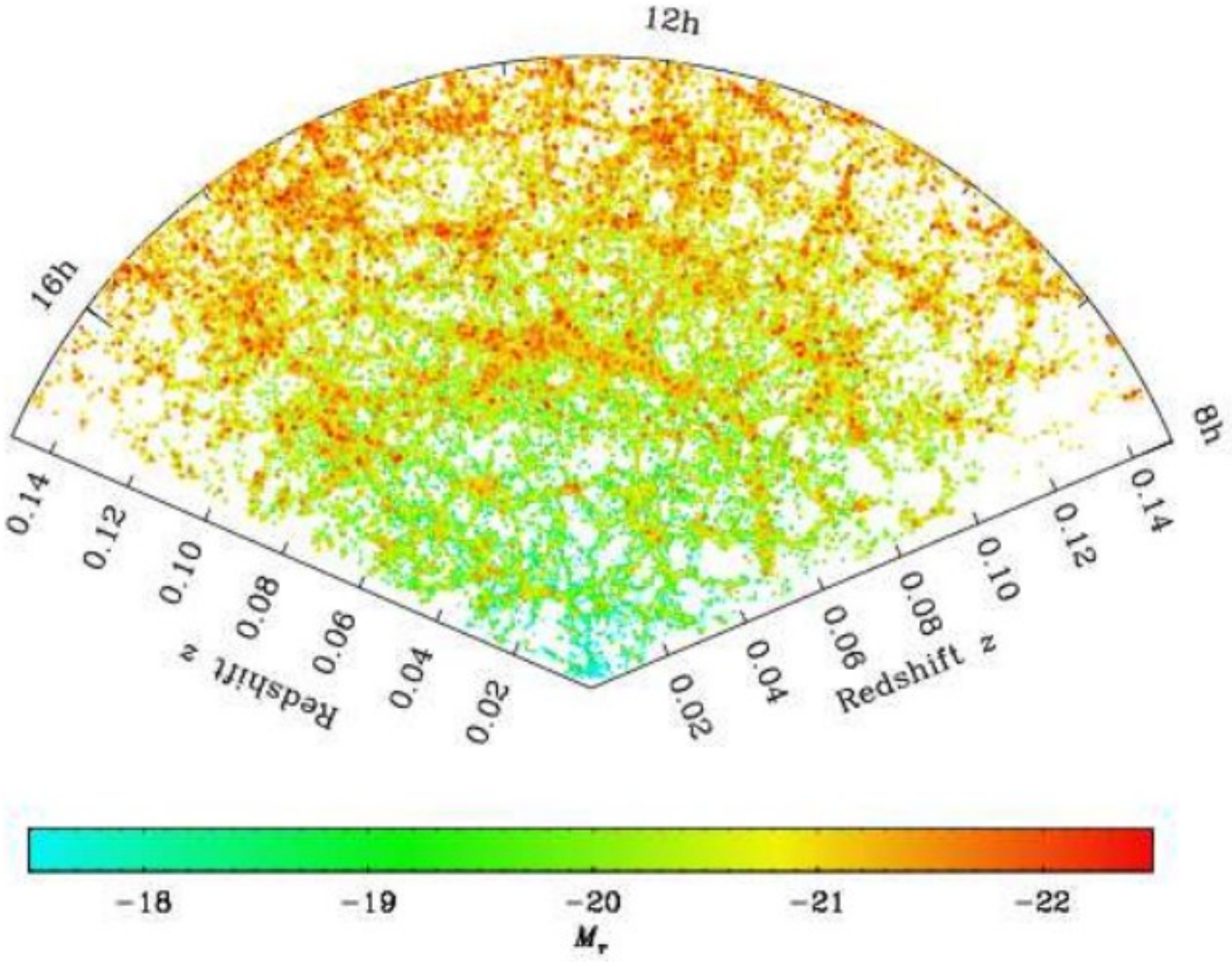

FIG. 3.— Like Figure 2, but with galaxies color-coded by absolute magnitude. The size of the dots is also proportional to galaxy luminosity. As expected for a flux-limited survey, more luminous galaxies dominate at larger redshifts.

Redshift-space distortions, a tool for statistical dynamics

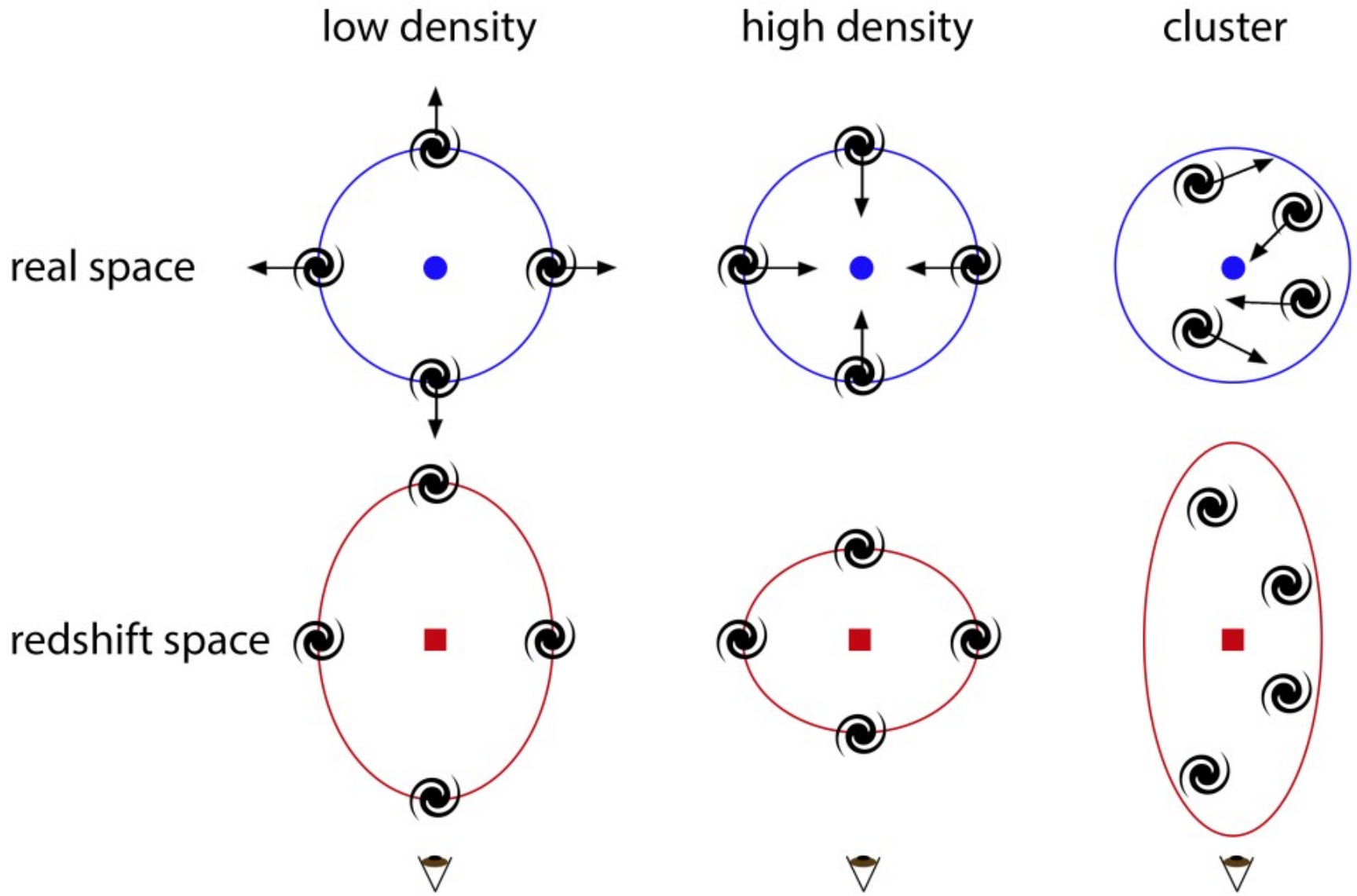

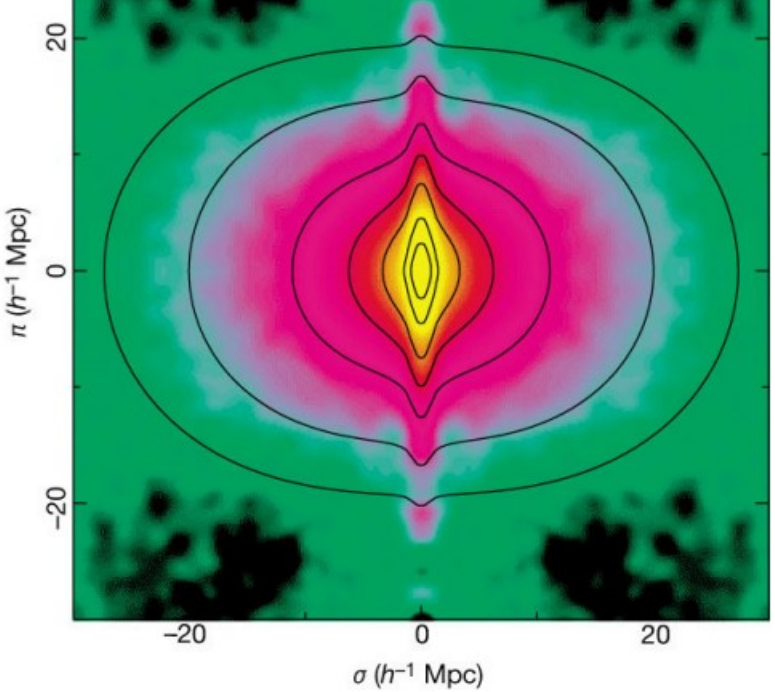

Figure 19: Measured redshift-space correlation function $\xi^{(z)}(s_\parallel, s_\perp)$ from the 2dFGRS survey (here $s_\parallel, s_\perp$ are called π, σ). Note that $s_\perp$ is positive by definition, since it's the radial coordinate of a cylindrical coordinate system. Likewise $s_\parallel$ is positive, since the separation $\mathbf{s}$ of a pair is only defined up to a sign. Here the plot is just reflected with respect to the middle vertical and horizontal to produce a more pleasing image. One can imagine a rotation around this vertical to represent the angular coordinate of which $\xi^{(z)}$ is assumed to be independent. The resulting 3D image gives the expectation value of the overdensity around a galaxy in redshift space. From Peacock et al.[30]

$$\sigma = D_{\mathrm{M}}(z')\ \theta$$

$$\pi = |\chi(z) - \chi(z')|$$

Information on the dynamics of galaxy structures !

Red galaxies dominated by virialized motions

Blue galaxies show strong infall pattern

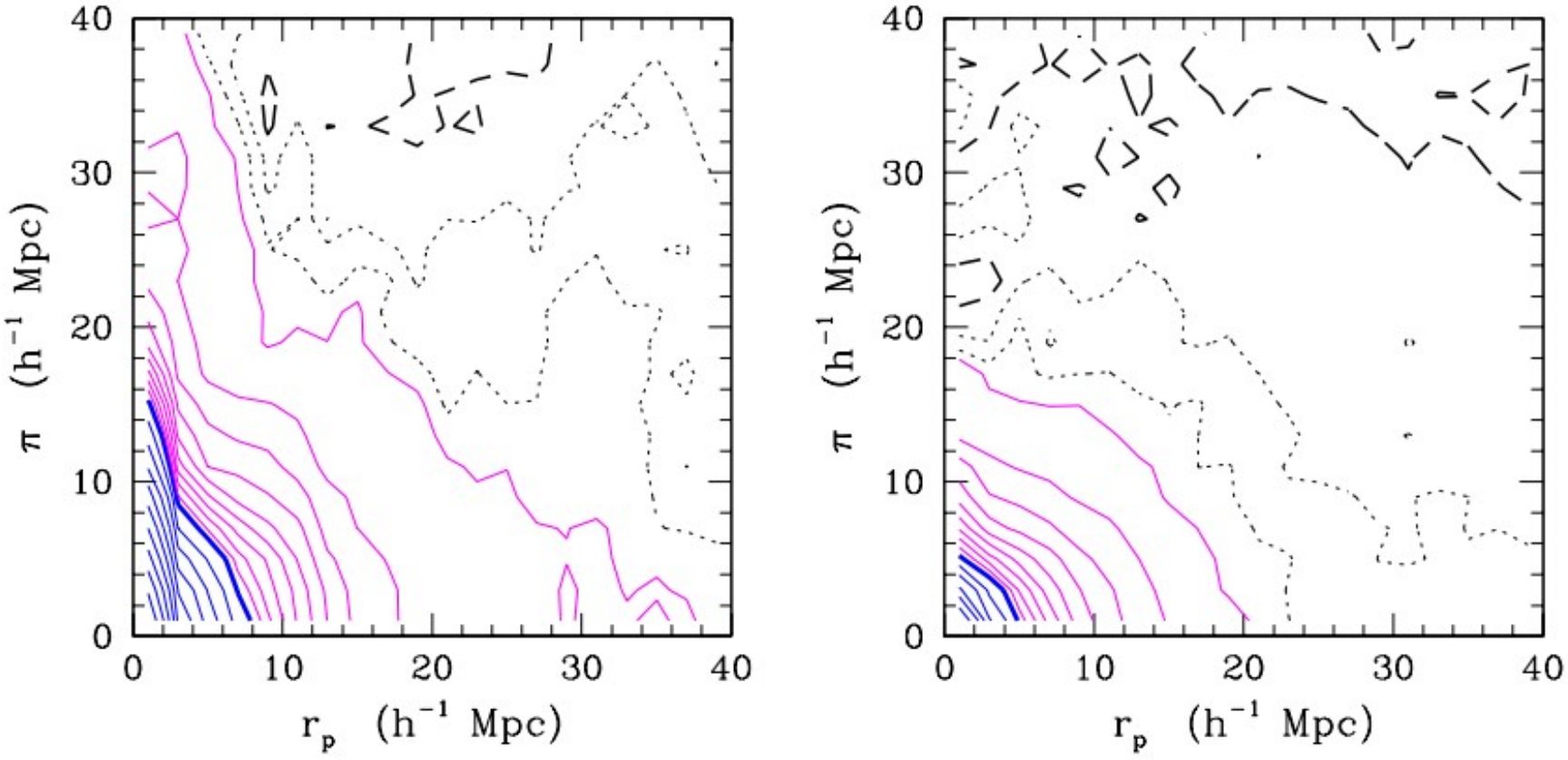

$$w_p \equiv \int_{-\infty}^{\infty} \xi(r_p, \pi) \mathrm{d}\pi \approx 2 \times \int_{0}^{\pi_{\mathrm{max}}} \xi(r_p, \pi) \mathrm{d}\pi$$

Zehavi et al. 2013

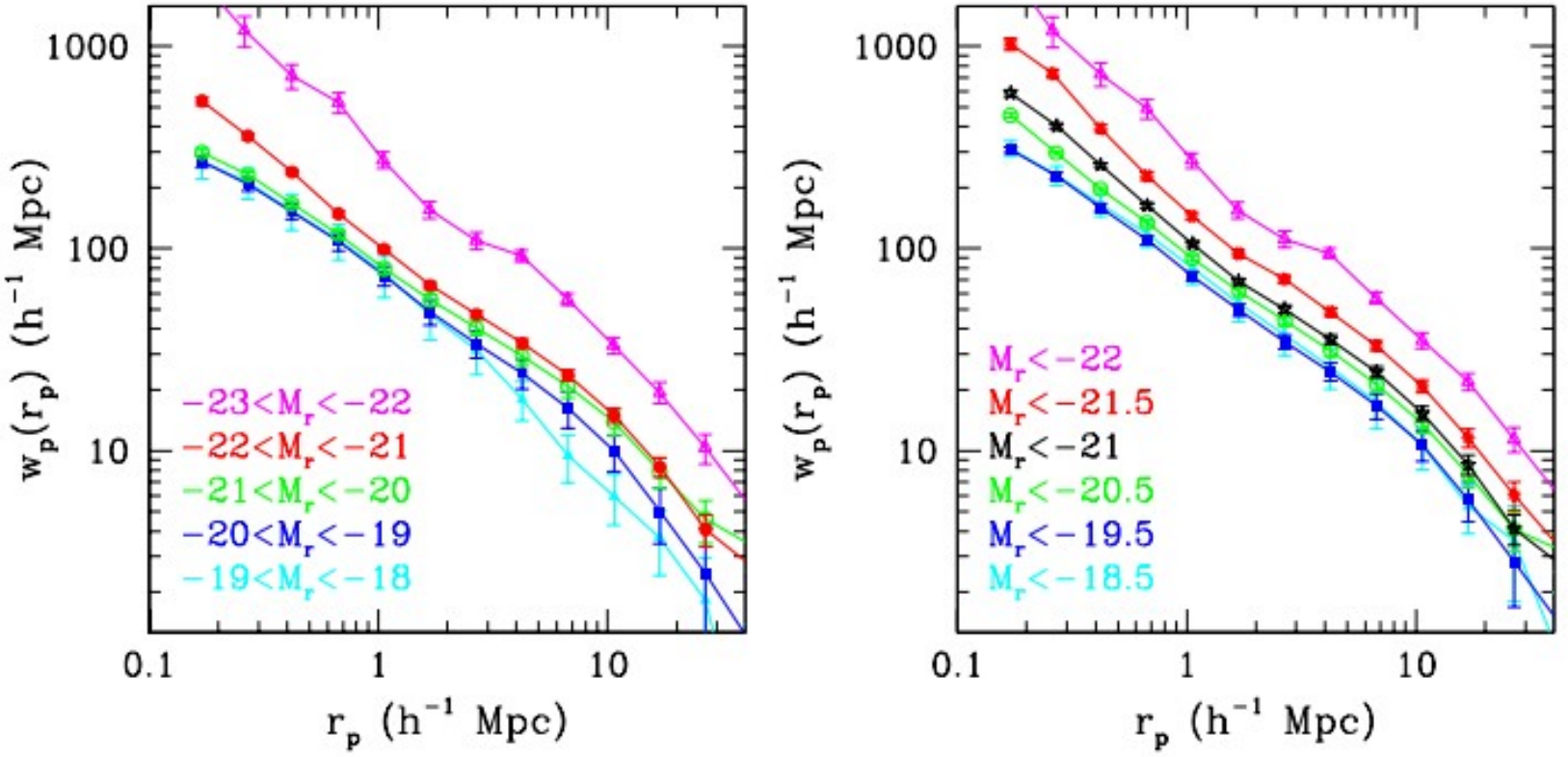

Models reasonably reproduced the main observed features in the data: two halo terms + FOG and infall pattern.

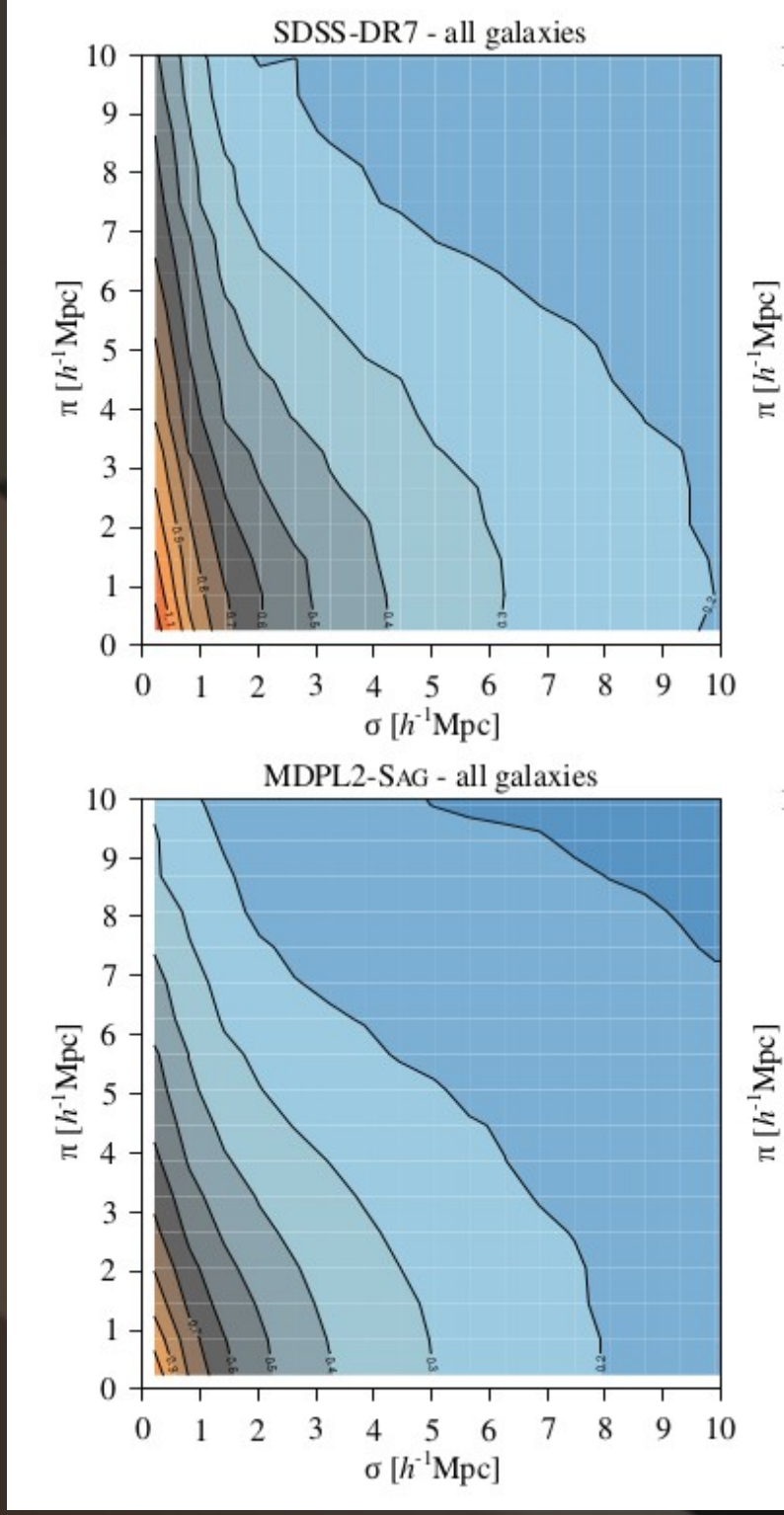

At large scales, before homogeneity is reached the BAO peak is a remarkable observed feature !

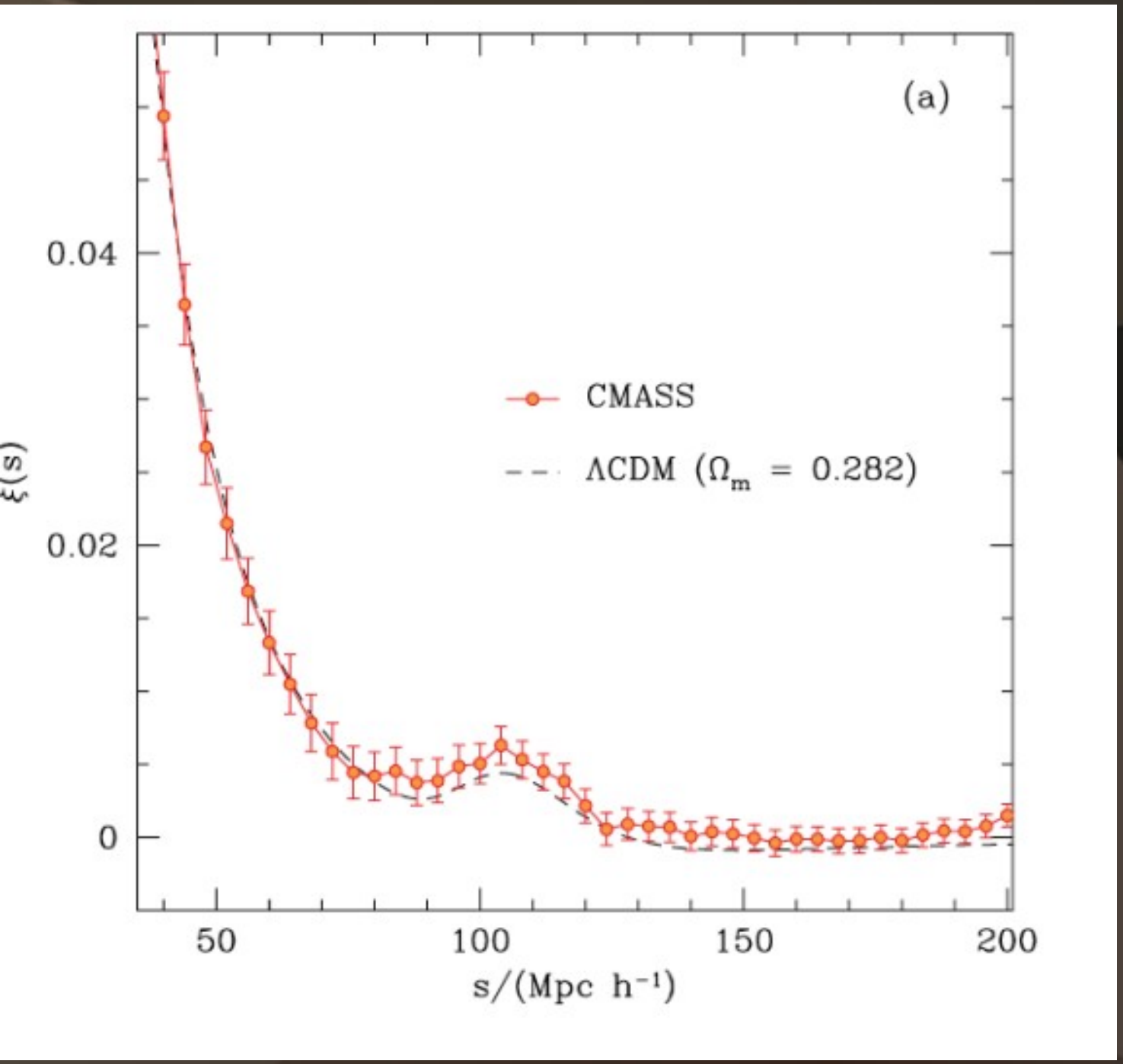

High precision correlation function

Possible more information will be obtained from new detailed statistical measures on present and future data.

Obrigado !